Journal of Materials Chemistry C

Accepted Manuscript

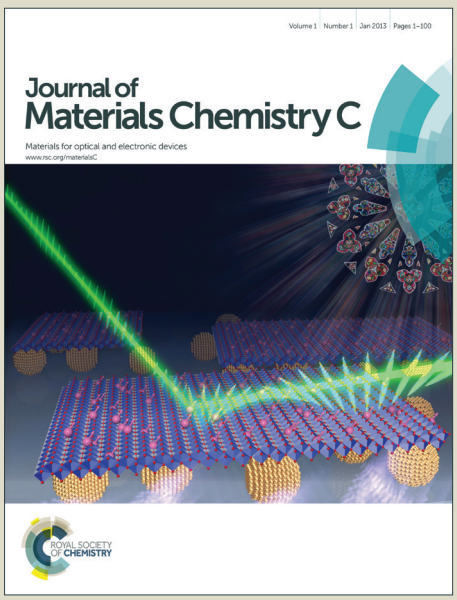

This is an *Accepted Manuscript*, which has been through the Royal Society of Chemistry peer review process and has been accepted for publication.

Accepted Manuscripts are published online shortly after acceptance, before technical editing, formatting and proof reading. Using this free service, authors can make their results available to the community, in citable form, before we publish the edited article. We will replace this *Accepted Manuscript* with the edited and formatted *Advance Article* as soon as it is available.

You can find more information about *Accepted Manuscripts* in the Information for Authors.

Please note that technical editing may introduce minor changes to the text and/or graphics, which may alter content. The journal's standard Terms & Conditions and the Ethical guidelines still apply. In no event shall the Royal Society of Chemistry be held responsible for any errors or omissions in this *Accepted Manuscript* or any consequences arising from the use of any information it contains.

ROYAL SOCIETY OF CHEMISTRY

www.rsc.org/materialsC

Properties and structural investigation of gallophosphate glasses by ^{71}Ga and ^{31}P nuclear magnetic resonance and vibrational spectroscopies

Patricia Hee,[1,2] Randi Christensen,[3] Yannick Ledemi,[2] John C. Wren,[3] Marc Dussauze,[4] Thierry Cardinal,[1] Evelyne Fargin,[1] Scott Kroeker[3*] and Younès Messaddeq[2*]*

(1) Institut de Chimie de la Matière Condensée de Bordeaux, CNRS-Université Bordeaux 187 Av. Dr. Schweitzer, 33608 Pessac, France

(2) Centre d'optique, photonique et laser, Université Laval Pavillon d'Optique-photonique 2375 rue de la Terrasse, Québec G1V 0A6, Canada

(3) Department of Chemistry, University of Manitoba, Winnipeg, MB, R3T 2N2, Canada

(4) Institut des Sciences Moléculaires, Université Bordeaux 1, CNRS UMR 5255, Bâtiment A12, 351 cours de la libération, 33405 Talence cedex, France

Abstract

The structure and optical properties of new gallophosphate glasses in the pseudo-binary system xGa_2O_3 – (100-x) $NaPO_3$ (x = 0 to 30 mol%), have been investigated. The effect of the progressive addition of Ga_2O_3 on the local glass structure has been evaluated using Raman and infrared spectroscopies, and ^{71}Ga and ^{31}P magic angle spinning nuclear magnetic resonance (MAS NMR) spectroscopy. ^{71}Ga MAS NMR spectra collected at ultrahigh magnetic field (21.1 T) and fast spinning rates (60 kHz) permit the quantification of gallium in 4-, 5- and 6-fold coordination as a function of the Ga_2O_3 concentration. At low concentrations of Ga_2O_3, high-coordinate gallium coordinates to oxygens associated with the phosphate chains, increasing the dimensionality and strengthening the glassy network. At moderate Ga loadings, tetrahedral Ga is incorporated into the phosphate chains, introducing additional branching sites which further enhances network connectivity. Higher Ga_2O_3 content results in the formation of Ga-O-Ga bonds, thereby inhibiting glass formation. ^{31}P MAS NMR and Raman and infrared spectroscopies provide complementary information about the distribution and connectivity of the phosphate groups within the glass network, supporting a structural model which is correlated with the

Journal of Materials Chemistry C Accepted Manuscript

measured optical and thermal properties of the Ga_2O_3-$NaPO_3$ glasses as a function of the Ga_2O_3 concentration.

TOC Summary and Graphic

Patricia Hee, Randi Christensen, Yannick Ledemi, John C. Wren, Marc Dussauze, Thierry Cardinal, Evelyne Fargin, Scott Kroeker and Younes Messaddeq

J. Mater. Chem. C **2014,** *xx*, xxxx

Properties and structural investigation of gallophosphate glasses by ^{71}Ga and ^{31}P nuclear magnetic resonance and vibrational spectroscopies

Progressive addition of Ga_2O_3 to a vitreous $NaPO_3$ network results in the continuous replacement of 6-fold by 4-fold coordinated Ga^{3+}, as clearly quantified by NMR and vibrational spectroscopies and correlated with the physical properties of the glasses.

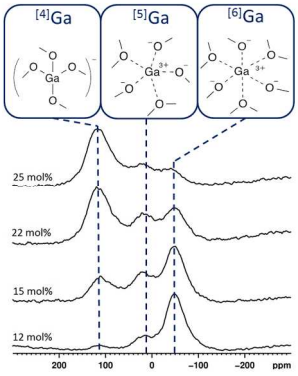

Journal of Materials Chemistry C Accepted Manuscript

1- Introduction

Phosphate glassy materials have been intensively studied for optical and biomedical applications over the past several decades.[1-3] In particular, aluminophosphate glasses have attracted special interest for optical applications such as lasers, owing to their high rare-earth ion solubility and excellent physical-chemical properties with respect to well-known silicate glasses.[4,5] Phosphate glasses generally possess low melting, softening and glass transition temperatures, facilitating their fabrication and shaping and large-scale manufacturing has been successfully implemented.[5] However, the main disadvantage usually encountered with phosphate-based glasses is their limited chemical durability, which may restrict practical applications. The addition of Al_2O_3 to form aluminophosphates improves their chemical durability[6] and has become the foundation of many useful glassy materials.

In the relentless drive toward device miniaturization, the replacement of gallium for aluminum is a key strategy by which glass refractive indices may be increased, allowing for higher numerical apertures and strong confinement of light in waveguide mode for integrated optoelectronics while maintaining high rare-earth (RE) solubilities.[7,8] A high concentration of well dispersed RE ions in glass is essential for designing shorter optical components in waveguides for photonic applications.[9] Arai et al. have demonstrated that the incorporation of aluminum into silica increases the rare-earth ion solubility[10] and gallium has been used similarly to enhance RE solubility in chalcogenide glasses.[11] The replacement of Al^{3+} by the larger Ga^{3+} may open up the network to better accommodate rare-earth ions. Moreover, the glass-forming region in gallophosphates is wider than in aluminophosphates, approaching the crystalline $GaPO_4$ composition. It is also expected that the incorporation of Ga_2O_3 into phosphate glasses will enhance their chemical durability,[12] improving the performance of devices developed from such glasses. Thanks to the high solubility of silver ions in gallium phosphate glasses, photochemistry can also be exploited for micro- and nano-structuring.[12,13] The higher hyperpolarizability of Ga^{3+} with respect to Al^{3+} also increases the possibility of accessing non-linear optical properties such as the Kerr effect or second-order non-linearity, while maintaining an absorption edge far into the UV region.[14]

Despite the many potential advantages of gallophosphate glasses in optical applications, few studies have been conducted on Ga_2O_3-based phosphate glasses (see below). Our examination of the structure of gallophosphate glasses by ultrahigh-field NMR is a critical first step to realizing

Journal of Materials Chemistry C Accepted Manuscript

the promise of these new materials. The correlation of optical properties with the structural characteristics of the glass is basic information fundamental to developing applications which exploit the aforementioned properties of gallium. In this work, we begin with an investigation of the base gallophosphate glasses because the use of NMR is generally incompatible with highly paramagnetic systems.

The local structure of phosphate glasses has been widely investigated and it is well established that phosphorus ions occupy tetrahedral sites, leading to four configurations commonly labeled Q^0 (i.e., PO_4^{3-}) to Q^3 (i.e., $PØ_3O$), where the index 0 to 3 represents the number of bridging oxygen (Ø) between two phosphorus ions and "O" is used to denote a non-bridging oxygen.[15] Glasses belonging to the pseudo-binary Ga_2O_3-P_2O_5 have been characterized by vibrational spectroscopy (Raman and Fourier-transform IR), suggesting that Ga^{3+} is mainly found in fourfold coordination.[16] For Ga_2O_3 content lower than 30 mol%, these glasses may be considered metaphosphates, close to $Ga(PO_3)_3$ and composed of phosphate chains interconnected by GaO_6 octahedra. For higher Ga_2O_3 content up to 40 mol%, which is the limit of glass-forming domain by melt-quench methods, gallophosphate glasses can be considered as pyrophosphates close to $Ga_4(P_2O_7)_3$, consisting of pyro-, ortho- and polyphosphate groups linked through GaO_4.[16] Structural studies on glasses belonging to the pseudo-ternary Ga_2O_3-Na_2O-P_2O_5 system have reported gallium ions in four-, six- and possibly five-coordination, with octahedral Ga predominating.[17,18] This conclusion is supported by analogy to aluminophosphate glasses, where ^{27}Al magic-angle-spinning (MAS) NMR spectroscopy has revealed appreciable amounts of these three coordination environments in sodium aluminophosphate glasses.[19] In that work, Brow et al. discussed their respective structural roles with reference to the bulk glass properties, suggesting that the common designations of glass "former" and "modifier" are of limited usefulness in these systems.

Solid-state NMR is particularly applicable to the study of short-range order (SRO) in oxide glasses, probing the local structural environments about spin-active nuclei such as ^{27}Al, ^{31}P, ^{23}Na and ^{17}O to obtain coordination numbers and, in favorable cases, next-nearest neighbor connectivity.[20-22] Nevertheless, despite the chemical similarities between gallium and aluminum, probing ^{71}Ga or ^{69}Ga by NMR in disordered materials remains more challenging than studying ^{27}Al due to its large quadrupolar interaction ($Q = 0.11\text{x}10^{-28}$ m^2), which can result in broad and featureless spectra.[17,23,24] A game-changer for solid-state ^{71}Ga NMR is the availability of

Journal of Materials Chemistry C Accepted Manuscript

ultrahigh-field magnets of 21.1 T (i.e., 900 MHz ^{1}H frequency) combined with ultrafast magic-angle-spinning probes capable of rotation rates up to 65 kHz. Together, these offer new possibilities for the direct observation of structurally informative ^{71}Ga MAS NMR spectra.[25]

In this work, gallophosphate glasses with compositions $x(Ga_2O_3) – (100\text{-}x)NaPO_3$ (x = 0 to 30 mol%) are studied to evaluate the role adopted by Ga_2O_3 in the sodium metaphosphate glass network. The local structure is characterized using vibrational spectroscopy (Raman and infrared), ^{71}Ga and ^{31}P MAS NMR. The ^{71}Ga MAS NMR spectra of the glasses were recorded at ultrahigh magnetic field (21.1 T), enabling unprecedented resolution of different Ga coordination environments in an oxide glass. Physicochemical properties such as density, the glass transition and crystallization temperatures, UV-Vis cut-off wavelength and linear refractive indices are also investigated and discussed with respect to the structural evolution of the glassy network as a function of gallium oxide content.

2- Experimental methods

2.1- Glass preparation

Glasses with nominal composition $(Ga_2O_3)_x$ - $(NaPO_3)_{100\text{-}x}$ (x = 0, 5, 10, 15, 20, 25, 27.5, 30) were prepared by the traditional melt-casting technique from commercial sodium hexametaphosphate (Sigma-Aldrich, analytical grade) and gallium oxide (Sigma-Aldrich, 99.99%). Glass samples are denoted as Ga*x* with *x* representing the content of gallium oxide in the glass (in mol%). The weighed and mixed raw materials were melted and fined in platinum crucibles in air for 30 minutes at temperatures ranging from 1000°C to 1400°C depending on the amount of gallium oxide. The melts were poured into stainless steel molds preheated to 40°C below the glass transition temperature, annealed for 6 hours at the same temperature and finally cooled slowly to room temperature. All glasses were colourless, transparent and bubble-free. The glass samples were cut and polished on both parallel faces for optical characterization.

2.2- Structural characterization

Elemental analysis was performed on the prepared samples using Inductively Coupled Plasma Optical Emission Spectroscopy (ICP-OES 720ES, Varian). The reported relative elemental quantities are averaged values from three measurements. The glass transition temperature, T_g, and crystallization onset temperature, T_x, were determined by differential scanning calorimetry (DSC)

Journal of Materials Chemistry C Accepted Manuscript

using a Netzsch DSC Pegasus 404F3 apparatus on glass pieces sealed in Al pans at a heating rate of 10˚C/min and with a precision of ± 2˚C. The density, ρ, was determined at room temperature by the Archimedes method with an Alfa-Mirage MD-300S densimeter using deionized water as immersion liquid. The measurement precision is estimated to be ±0.01 g/cm^3. UV-visible transmission spectra were recorded on a Cary 50 (Varian) spectrophotometer. Linear refractive index was measured by employing the M-lines prism coupling technique (Metricon 2010) at 532, 633, 972, 1308 and 1538 nm wavelengths with an accuracy of ± 0.002.

Raman spectra were recorded using a LABRAM 800HR Raman spectrometer (Horiba Jobin Yvon) and the 532 nm line of an Argon ion laser (Melle Griot). No interaction between the material and the focused laser beam was observed.

The IR spectra were recorded on a Bruker Vertex 70v spectrometer equipped with DTGS detectors and two beam splitters (KBr or mylar multilayer). A total of 200 scans was averaged with a resolution of 4 cm^{-1}. Reflectance experiments were performed using an external reflection attachment (Graesby, Specac) at an incident angle of 12^o. Absorbance spectra were calculated from the reflectance spectra by the Kramers-Kronig analysis.[26,27]

^{71}Ga MAS NMR spectra of ground glass samples were collected on a Bruker Avance II 900, using at 21.1 T magnet with a 1.3 mm Bruker MAS probe. Single-pulse experiments were performed using a small tip angle of 15˚ (ν_{rf} = 123 kHz) to ensure quantitative excitation, while the samples were spun at the magic angle at 60 kHz. Spectra are composed of 5 to 10 thousand co-added transients collected with an optimized recycle delay of 5 seconds (7 – 14 hour collection times). Spectral lineshapes were fit using DMfit2011[28] employing the "CZsimple" model,[29] a simplified version of the Czjzek distribution which accounts for distributions in the chemical shift and quadrupolar parameters.

^{31}P MAS NMR spectra were collected on a Varian ^{UNITY}Inova 600 with a 14.1 T Oxford magnet and a 3.2 mm Chemagnetics MAS probe. Single-pulse experiments were performed with a 90^o pulse at a spinning rate of 12 kHz. Spectra are composed of 16 co-added transients with an optimized recycle delay of 100 seconds. All the experiments were performed at room temperature.

3- Results

3.1- Physical-chemical properties

Journal of Materials Chemistry C Accepted Manuscript

The glass compositions measured by ICP-OES are reported in Table 1 along with the batch compositions and the Ga_2O_3/P_2O_5 and Na_2O/P_2O_5 ratios. No significant phosphate (P_2O_5) losses during glass preparation are observed. However, some deviation from the nominal composition is evident by comparing the theoretical and experimental and Ga_2O_3/P_2O_5 ratios when increasing the Ga_2O_3 content in the glass. This may be attributed to the increase in temperature from 1000 to 1400˚C required to achieve complete glass melting with higher Ga_2O_3 loading and may lead to metaphosphate evaporation. For a better understanding of the structure-property relations, only the measured compositions will be considered in the text, i.e., the samples constituting the glass series are denoted: Ga0, Ga5, Ga12, Ga15, Ga22, Ga25, Ga29 and Ga32.

The densities measured for the gallophosphate glass samples are shown in Figure 1a. The values increase with increasing Ga_2O_3 concentration in the glasses, as expected. Subtle undulations in the data imply different compositional regions. Upon the initial addition of 5 mol% Ga_2O_3 the density increases rapidly with respect to the pure sodium phosphate glass, after which the increase is slightly less pronounced. Above 25 mol% smaller increases are observed, suggesting saturation-like evolution.

Figure 1b shows the effect of Ga_2O_3 content on the glass transition temperature (T_g), the crystallization onset temperature (T_x) and the evolution of the thermal stability against crystallization ($\Delta T=T_x-T_g$). T_g increases from 295°C for the Ga_2O_3-free glass sample up to 460°C for Ga32. Two linear regions with similar slopes can be identified in the T_g data: from 0 to 15 mol% and from 22 to 32 mol%, with an offset between these lines. An alternate way to view the data is in terms of three compositional regions: a rise from 0 to 12 mol% followed by a plateau from 12 to 22 mol%, and finally another rise from 22 to 32 mol%. This latter perspective is reminiscent of subtle trends in the density data. T_x follows roughly the same pattern as a function of Ga_2O_3 concentration, implying little variation in ΔT, which ranges between 50 to 80˚C across the full range of Ga_2O_3 loading.

Figure 2a presents the absorption coefficient spectra of the Ga_2O_3-$NaPO_3$ glasses in the UV-visible range. For an absorption coefficient α = 10 cm^{-1}, which is a commonly used value to define the glass cut-off wavelength (in the Urbach regime), the corresponding wavelengths fall within a small range between 284 and 291 nm and do not evolve with the Ga_2O_3 content, indicating that Ga has no significant influence on the optical band gap. One can however notice the presence of an absorption band near 250 nm which is more prominent for the glasses with

Journal of Materials Chemistry C Accepted Manuscript

lower concentration of gallium oxide. This absorption band may be attributed to the presence of contaminants such as transition-metal ions present in the sodium hexametaphosphate starting material. Trace transition metal impurities in glasses are known to strongly absorb in the UV range.[30]

The refractive indices measured on the glass samples at five wavelengths are presented in Figure 2b as a function of Ga_2O_3 concentration, where the same increasing trend in refractive index at each wavelength is evident. This increase is related to the addition of comparatively heavy Ga^{3+} ions in the glass network. A slight inflection can be observed between 15 and 25 mol% Ga_2O_3, reminiscent of the behaviour noted in the evolution of characteristic temperatures and density as a function of Ga_2O_3 content.

3.2- Glass structure

Phosphate-based glasses comprise a short-range ordered network of tetrahedral PO_4 units. These structural units can be thought of as having one doubly bonded oxygen while the remaining three oxygens are either covalently bonded to another tetrahedron ("bridging oxygens", Ø) or coordinated through electrostatic effects to an adjacent cation. The variation in these units may be described by the Q^j nomenclature, where j = 3, 2, 1 or 0 and represents the number of singly bonded oxygens that form covalent bonds to other phosphorus ions, as depicted in Figure 3.[15] The progressive addition of a modifier, e.g. sodium oxide, to the phosphate glass results in network depolymerization, converting Q^3 units ($PØ_3O$) into Q^2 units ($PØ_2O_2^-$) when $0 < Na/P \leq 1$ or O/P = 3. At Na/P = 1, the resulting network consists, to a first approximation, of one-dimensional polymerized chains of Q^2 units. In the $1 \leq Na/P \leq 2$ or O/P = 3.5 range, Q^1 units ($PØO_3^{2-}$) replace Q^2 units, terminating the Q^2 chains and resulting in shorter molecular fragments. The network is further depolymerized when isolated Q^0 replace Q^1 units at $O/P \geq 4$ or $2 \leq Na/P \leq 3$.

As gallium is a group 13 element directly below aluminum in the periodic table, it has been found that the local structure of gallium in oxide glasses often behaves analogously to that of aluminum.[31,32] Both aluminum and gallium oxides are considered to be intermediate glass formers, meaning they cannot form a glass on their own, but can act as a modifiers or glass formers in the presence of other glass-forming elements, adopting coordination numbers of $^{[j]}$Ga, where j = 4, 5, 6. High-coordinate gallium species ($^{[6]}$Ga and $^{[5]}$Ga) are considered to function

Journal of Materials Chemistry C Accepted Manuscript

loosely as glass modifiers that are likely charge-compensated by a combination of bridging and non-bridging oxygens between phosphorus or gallium, as shown in Figure 3, whereas $^{[4]}$Ga is in nominally tetrahedral coordination which is usually favorable for glass-forming.[32,33]

As the samples studied here are primarily ternary glasses, a more elaborate classification scheme must be used to define longer-range connectivity: Q_m^n, where *n* represents the number of phosphorus next-nearest neighbors and *m* represents the number of gallium next-nearest neighbors. Note that this scheme does not specify whether adjacent gallium ions are covalently bound or interacting principally through electrostatic forces, as expected for high-coordinate Ga.

3.2.1- Vibrational spectroscopy

Figures 4a and 4b show the Raman and infrared spectra recorded for the gallophosphate glasses. The vibrational spectrum of "Ga0" (i.e., $NaPO_3$ glass) has been described in the literature.[34,35] In the Raman spectrum, the main bands centered near 1150 and 690 cm^{-1} have been assigned respectively to Q^2 ($P\O_2O_2$) symmetric stretching vibrations associated with terminal oxygen species and symmetric P-O-P bond stretching vibrations with phosphorus atoms in Q^2 tetrahedra.[12,16-18] According to Velli et al., the band at about 1270 cm^{-1} in the IR spectrum can be attributed to Q^2 and Q^3 units. A band can be observed near 1150 cm^{-1} and assigned to Q^2, but also a band at 1100 cm^{-1} to the asymmetric stretching mode of end groups of Q^1 ($\O PO_3$) units. Vibrations around 1010 cm^{-1} correspond to P-O-P asymmetric vibrations, and finally, the band at 880 cm^{-1} to asymmetric vibration of P-O-P chains with Q^2 units.[35]

The gradual addition of Ga_2O_3 into the $NaPO_3$ glassy network results in numerous spectral changes. In the high wavenumber range of the infrared spectra, the band around 1270 cm^{-1} for Ga0 shifts to 1200 cm^{-1} and then to 1150 cm^{-1} with the progressive introduction of gallium oxide. These changes result from the modification of the environment of the non-bridging oxygen of the Q^2 units and are directly related to the decrease in sodium, which act as modifier for the glassy network, and the appearance of gallium polyhedra acting as charge compensators.[36] In the Raman spectra of Ga12, a large shoulder appears close to 1230 cm^{-1} and shifts down to 1200 cm^{-1} in the spectra of the Ga_2O_3-rich compositions. This band was assigned to the stretching motions of the two non-bridging oxygens bonded to phosphorus in Q^2 tetrahedra.[15]

In the Raman spectra, the band observed at 1270 cm^{-1} for Ga0 and Ga5 can be attributed to the stretching mode of P=O bonds in Q^3 tetrahedra.[37] This band is no longer visible after 20% Ga_2O_3

Journal of Materials Chemistry C Accepted Manuscript

has been introduced. In the spectral range between 800 and 1150 cm^{-1} the addition of Ga_2O_3 into the glass network results in the appearance of a doublet at 1050 and 1100 cm^{-1} in the Raman spectra of Ga5 and Ga12. The band at 1050 cm^{-1} can be ascribed to the symmetric vibration of Q^1 species[12] while the band at 1100 cm^{-1} is attributed to the symmetric vibration of Q^2 species[12] but also to the asymmetric vibrations of Q^1 species.[15] For Ga15, the band at 1050 cm^{-1} becomes dominant and for the Ga15 to Ga32 samples, this vibration shifts up to nearly 1000 cm^{-1} when the Ga_2O_3 content is increased. Regarding the infrared spectra, the band around 1100 cm^{-1}, attributed by Velli et al. to the asymmetric stretching mode of Q^1 end groups, decreases progressively as gallium oxide is introduced and is no longer visible above 20% of Ga_2O_3.[35] The band between 900 cm^{-1} and 1000 cm^{-1} is related to P-O-P bonds. One can observe that the band around 880 cm^{-1} attributed to long chains shifts to the high wavenumber range and is no longer visible in Ga29. In the Raman spectra, the 920 cm^{-1} band can be attributed the asymmetric vibrations of P-O-P bonding.[12,15,17,18] This vibration is not visible above 20 mol% of Ga_2O_3. For high gallium oxide loading (Ga29 and Ga32) the two main bands in this spectral range are located around 1010 cm^{-1} and 1050 cm^{-1} and correspond to the vibrations respectively of P-O-P bonds and end groups of Q^1 units.

Regarding the vibrations below 800 cm^{-1} in the Raman spectra, the bands at 750 cm^{-1} and 350 cm^{-1} were assigned to the symmetric stretching of the P-O-P bond with phosphorus atoms in tetrahedral Q^1 units and to the vibration of GaO_6 octahedra, respectively.[16,38,39] The vibration at 750 cm^{-1}, attributed to the presence of Q^1 units, increases when Ga_2O_3 is incorporated into the matrix up to a maximum intensity of 15 mol% and then rapidly decreases in Ga20 and Ga22. For more than 15 mol% Ga_2O_3, the band attributed to P-O-P vibrations in long phosphate chains at 690 cm^{-1} has almost vanished. The Raman and IR spectra of Ga32, Ga29 and Ga25 appear to be very similar, except for the slight shifts indicating a stabilization of the quantity of Q^2 and Q^1 units.

Several groups have attributed vibration at 640 cm^{-1} in the Raman spectra to vibrational modes of GaO_4 tetrahedra.[17,18,38-40] In figure 4a, this band can be seen to appear in the Ga15 spectrum and seems to split into two bands with further addition of Ga_2O_3. Fukunaga et al have assigned the Raman peak at 500 cm^{-1} to a bending mode of GaO_4;[40] this peak grows with Ga loading, consistent with ^{71}Ga MAS NMR data indicating increasing four-coordinate gallium (*vide infra*). In the infrared spectrum, bands between 640 cm^{-1} and 660 cm^{-1} have been associated with

Journal of Materials Chemistry C Accepted Manuscript

vibrational modes of GaO_4 tetrahedra. Vibrations of six-coordinate Ga^{3+} ions are reported by Miyaji et al. between 500 cm^{-1} and 600 cm^{-1} [41]. According to figure 4b, a shoulder at around 590 cm^{-1} can be observed in the infrared spectrum for the sample Ga5, Ga12 and Ga15 and vanishes at the highest Ga_2O_3 content. Assignment in this spectral range is not obvious, although Pickup at al reported in gallium phosphate glass that vibration around 590 cm^{-1} could be attributed to O-P-O deformation modes.[42]

3.2.2- ^{71}Ga MAS NMR spectroscopy

The ^{71}Ga MAS NMR spectra of the glass samples are presented in Figure 5. Each spectrum shows the presence of three broad and overlapped resonances, with composition-dependent intensities. At 5 mol% Ga_2O_3, the main peak is centered around -40 ppm, with two smaller peaks at about 20 and 100 ppm. Based on previous ^{71}Ga NMR measurements of four- and six-coordinate gallium[43,44] and the correlation between ^{27}Al and ^{71}Ga documented by Bradley[45] and Massiot,[46] the highest frequency peak can be assigned to $^{[4]}$Ga, the lowest frequency peak to $^{[6]}$Ga, and the peak in the middle to $^{[5]}$Ga. With the continuous addition of Ga_2O_3, the peak intensity of $^{[4]}$Ga increases while that of $^{[6]}$Ga decreases. The $^{[5]}$Ga peak intensity remains relatively constant with Ga_2O_3 additions, relative to the total ^{71}Ga NMR signal. Above 25 mol% Ga_2O_3, only minor spectral changes are observed.

The Czjzek distribution function was used to reproduce peak shapes under the dual effects of electric-field gradient and chemical shift distributions (Figure 6a). By determining the area under each peak, the fraction of each Ga SRO unit in the glass was estimated with respect to the total ^{71}Ga NMR signal (Figure 6b). The number of $^{[6]}$Ga decreases rapidly from 79 to 11% of the total Ga with increasing Ga_2O_3 content, until Ga_2O_3 > 25 mol%. The inverse trend is observed for $^{[4]}$Ga, its concentration increasing from 5 to 68% over the same compositional range. The number of $^{[5]}$Ga SRO units changes more gradually, varying from 16% at 5 mol% Ga_2O_3 to 27% at 15 mol% Ga_2O_3. These trends are essentially arrested at Ga_2O_3 contents higher than 25 mol%, where all three structural units undergo small changes.

Another way to visualize the data is to plot the fraction of Ga polyhedra with respect to the total number of gallium and phosphorus polyhedra (Figure 6c). As such, it may be observed that $^{[6]}$Ga appears to oscillate about 4 – 9% of the total SRO units in the glass, with three regimes corresponding roughly to 0 – 12, 12 – 25, and 25 - 32 mol% Ga_2O_3 reminiscent of the regions

Journal of Materials Chemistry C Accepted Manuscript

detected in the T_g data (Figure 1b). $^{[4]}$Ga content follows similar compositional ranges, with the strongest increase corresponding to the decrease in $^{[6]}$Ga. $^{[5]}$Ga increases steadily from near zero to 7%. This behaviour may be indicative of its role as a transition structure between four- and six-fold coordinate gallium, as postulated for $^{[5]}$Al and $^{[5]}$Si.[47-49]

In addition to the changing concentration profile of each structural unit, changes in their isotropic chemical shift can give information about the evolution of the glass network structure. Figure 6d shows that the isotropic chemical shift, δ_{iso}, obtained by Czjzek fitting, of all Ga polyhedra is relatively constant until approximately 20 mol% Ga_2O_3. At 22 mol% Ga_2O_3, δ_{iso} ($^{[4]}$Ga) shifts to a higher frequency and remains constant with increasing Ga_2O_3. The δ_{iso} values of $^{[5]}$Ga and $^{[6]}$Ga also shift to higher frequencies with increasing Ga_2O_3 above 25 mol% Ga_2O_3. Since the chemical shift of ^{71}Ga appears relatively insensitive to the effect of P next-nearest-neighbors (NNN), this small but distinct change in δ_{iso} may signal the introduction of Ga NNN in high-energy Ga-O-Ga linkages.

3.2.3- ^{31}P MAS NMR spectroscopy

The ^{31}P MAS NMR spectra can be seen in Figure 7. Because of significant spectral overlap in the peaks comprising most of these spectra and the multiple factors which can influence peak positions, they are best interpreted in the context of the unambiguous ^{71}Ga MAS NMR results. In the binary sodium phosphate glass (i.e., 0 mol% Ga_2O_3), the spectrum has peaks at 2 ppm and -17 ppm, which are readily identified from previous work on sodium phosphate glasses as Q^1 and Q^2, respectively.[15] This binary glass has a one-dimensional network made up of P-O-P 'chains' of Q^2 units terminated by Q^1. With the addition of Ga_2O_3, a new peak is observed at -7 ppm, which can be attributed to chain phosphorus modified by $^{[6]}$Ga in the second coordination shell, $Q^2_{1(6)}$, where the "1(6)" subscript indicates that phosphorus is near one $^{[6]}$Ga. Based on the logic of bond valence,[19] high-coordinate gallium is expected to coordinate to oxygen in the phosphate chain (bridging, non-bridging and doubly bonded) without any appreciable depolymerization. Hence, interaction with $^{[5/6]}$Ga appears to increase the chemical shift of Q^2 by about 10-12 ppm. Since each $^{[5/6]}$Ga is expected to interact with about three phosphorus atoms on at least two separate chains (see Figure 8), the chemical shifts of three P atoms will be modified by the addition of each Ga. At 5 mol% Ga_2O_3, the 10 Ga atoms added will influence about 30 P, which corresponds to about 32% of the P in the glass, in good agreement with the intensity of the peak at -7 ppm.

Journal of Materials Chemistry C Accepted Manuscript

At 12 mol% Ga_2O_3, almost all of the added Ga is in five- and six-fold coordination according to the ^{71}Ga MAS NMR, permitting the assumption that no appreciable phosphate depolymerization is occuring but that $^{[5/6]}$Ga link adjacent chains via electrostatic interactions with the chain oxygens. By the logic articulated above, the chemical shifts of about 85% of the P in the glass would be affected by the presence of high-coordinate Ga, consistent with the relative fitted intensities of the peaks at -7 and -20 ppm.

In the glass with 15 mol% Ga_2O_3, a significant fraction of the added gallium is present as four-coordinate species. Since Ga-O-Ga are likely to be energetically disfavored [32], $^{[4]}$Ga are expected to insert into the phosphate chains, initially forming $Q^1_{1(4)}$ units. Based on the ^{31}P chemical shift scheme inferred from aluminophosphate glasses on the basis of ^{27}Al-^{31}P double-resonance NMR experiments,[50-52] it appears that $Q^2_{1(5/6)}$ and $Q^1_{1(4)}$ are likely to have similar chemical shifts. A mass-balance calculation based on the assumption that all of the Ga is in high coordination leads to the conclusion that about 105% of the phosphorus will be shifted by interaction with $^{[5/6]}$Ga, implying that these "sites" are saturated and confirming that some Ga must begin to enter the chains as $^{[4]}$Ga. Essentially no evidence of Q^2_0 remains in the ^{31}P spectrum (-20 ppm), with the bulk of the intensity concentrated in a broad peak around -7 ppm, which likely represents Q^2 in close proximity to any form of Ga. There is a hint of intensity to high frequency of the Q^1 terminal phosphate units which may indicate that even these phosphorus units have Ga NNN.

The decrease in absolute $^{[6]}$Ga between 12-25 mol% Ga_2O_3 (Figure 6c) can be attributed to the corresponding decrease in phosphorus content, thereby depriving the high-coordinate Ga of bonding sites and forcing the added Ga to replace P in the chains. Correspondingly, in the glass with 22 mol% Ga_2O_3, most of the Ga is tetrahedral because there are no more bridging or non-bridging chain oxygens to accommodate high-coordinate Ga. This results in further high-frequency ^{31}P NMR shifts since there are essentially no P atoms which are not in close proximity to Ga either by bridging within chains ($^{[4]}$Ga) or by electrostatic interactions between chains ($^{[5/6]}$Ga). The spectrum likely contains contributions from multiple species which resonate at roughly the same frequencies, including $Q^2_{1(5/6)}$, $Q^1_{1(4)}$, $Q^0_{1(4)}$, $Q^1_{1(5/6)}$ and possibly even $Q^1_{1(4)}$ with additional $^{[5/6]}$Ga coordinated to the oxygens, thereby producing the broad undifferentiated ^{31}P MAS NMR peakshape in Figure 7.

The ^{31}P MAS NMR spectra of samples containing 25-32 mol% Ga_2O_3 consist of a single broad peak around 0 ppm, implying that all of the P is highly influenced by nearby Ga. Various

Journal of Materials Chemistry C Accepted Manuscript

species such as $Q^0_{2(4)}$ and $Q^1_{1(4)}$, likely further coordinated by $^{[5/6]}$Ga, contribute to this composite signal. The observation that these three spectra are practically indistinguishable despite increased Ga loading suggests that the phosphorus environments are "saturated" with Ga and no further local changes are possible about P above 25 mol% Ga_2O_3.

4- Discussion

4.1- Glass structure

In accordance with previous work,[53] the vibrational and NMR spectroscopic results indicate that the glass network begins as a binary sodium phosphate glass, composed of chains of Q_0^2 units with Q_0^1 units terminating the chains. Like aluminum, it may be assumed that gallium will avoid Ga-O-Ga connections if possible, particularly in the four-coordinated units where the negative charge accumulation at the interconnecting oxygen is disfavored by bond valence arguments [32]. Hence, the addition of 5-12 mol% Ga_2O_3 introduces high-coordinate gallium which interacts with phosphate chain oxygens, effectively increasing the dimensionality of the network by cross-linking the chains without appreciable depolymerization. As $^{[6]}$Ga and $^{[5]}$Ga make up approximately 95% of the gallium SRO units, bond valence dictates that these units are integrated into the network through weak electrostatic interactions as exemplified in Figure 8. This connectivity pattern is consistent with that found in the monoclinic form of $Al(PO_3)_3$ [54] and is further supported by the work of Zhang et al., which showed that in sodium aluminophosphate glasses with P/Al $\geq$ 4, all aluminum species interact equally with phosphorus, implying a high degree of Al proximity to phosphorus irrespective of Al coordination number.[52] The lack of Q_0^1 units in the vibrational and NMR spectra supports that the network is fully interconnected by the presence of gallium structural units.

At 15 mol% Ga_2O_3 the available "cross-linking" sites in the phosphate chains are saturated by high-coordinate Ga and the excess Ga must begin to replace chain phosphorus to avoid the formation of Ga-O-Ga bonds. This is reflected in the ^{71}Ga NMR data by a sharp increase in the fraction of four-coordinate Ga (Figure 6b). The decrease in the number of six-coordinate Ga (Figure 6c) is a consequence of the decrease in overall phosphorus content resulting in fewer cross-linking sites. A similar observation was made for the aluminum coordination number in aluminophosphate glasses by Brow,[6] who noted that the abrupt increase in $^{[4]}$Al occurs at the transition from the metaphosphate (O/P = 3.0) to pyrophosphate (O/P = 3.5) region. Indeed, the

Journal of Materials Chemistry C Accepted Manuscript

^{71}Ga NMR data shown in Figure 6b lead to a speciation plot which is remarkably similar to that presented by Bencoe et al.,[51] underscoring the close connection between the respective roles of Ga and Al in phosphate glasses.

At 22 mol%, where the P/Ga ratio is 1.78, $^{[4]}$Ga makes up the majority of the Ga structural units at 52%. Phosphate chains have been converted to gallophosphate chains with charge ordering. This is supported by the observation of further deshielding of the ^{31}P NMR peaks,[19] all of which are influenced by the proximity of Ga in the next-nearest neighbor positions. Local charge balance may be effected by two possible mechanisms. Strict P/Ga alternation, where phosphorus tetrahedra are surrounded by four bridging oxygens to form a cationic centre, may in principle satisfy the requirements of charge balance. In crystalline gallophosphates, aluminophosphates and borophosphates, such phosphorus species are found in characteristic shielding ranges to significantly higher frequency than the peaks observed here. Such three-dimensional ordering tends to produce clustering and renders the glasses prone to crystallization, which is not observed in these samples. More likely is that sodium cations displaced from NBOs by high-coordinate Ga associate with anionic $^{[4]}$Ga, leaving phosphorus species neutral. Making the common assumption that $^{[4]}$Ga do not bear nonbridging oxygens, the incorporation of Ga into the phosphate chains in this way further increases the interconnectivity of adjacent chains by the formation of four $^{[4]}$Ga-O-P linkages (see Figure 8). This analysis suggests that the vibrations observed in Raman and infrared spectroscopy around 1000 cm^{-1} correspond to vibrations involving P-O-$^{[4]}$Ga bonds.

For Ga_2O_3 contents greater than 25 mol%, the P/Ga ratio is 1.4 or less and the phosphorus environments are saturated by Ga NNN of variable coordination numbers, again following the observation of Brow et al. that transitioning from the pyrophosphate (O/P = 3.5) to orthophosphate (O/P = 4.0) region induces distinct structural changes.[6] Increasing the Ga_2O_3 content has no apparent influence on the ^{31}P NMR or vibrational spectra, indicating that the glass network consists of highly interconnected phosphate and gallate units. In particular, the IR and Raman spectral regions above 900 cm^{-1} do not evolve with increasing Ga, confirming that the maximum number of P-O-Ga bonds have been formed. The ^{71}Ga NMR spectra, however, reveal subtle changes in the peak positions (Figure 6d) which suggest that the excess added gallium forms Ga-O-Ga bonds. The apparent invariance of ^{71}Ga NMR peak positions from 5 – 22 mol% Ga_2O_3 indicates that ^{71}Ga NMR chemical shifts are not very sensitive to the number of P NNN.

Journal of Materials Chemistry C Accepted Manuscript

The small but significant shifts observed above 22 mol% may be interpreted as signifying the onset of other bonding partners. Moreover, the concentrations of $^{[5]}$Ga and $^{[6]}$Ga show a small increase at the expense of $^{[4]}$Ga, (Figure 6b) suggesting the quantity of $^{[4]}$Ga is being limited by the phosphorus content. As all P-O-Ga bond requirements suggested by the ^{31}P data are being filled by $^{[4]}$Ga, the high-coordinate gallate units must have primarily $^{[6/5]}$Ga-O-$^{[6/5]}$Ga bonds. The distinct Ga speciation behaviour in these compositions (Figure 6c) further supports the notion that all Ga species are increasing despite no further evolution of the phosphate network. Finally, the dissociation of gallium from the phosphate network and sequential formation of Ga-O-Ga bonds is likely related to the limit of glass-forming ability of these materials by melt-quench methods. Considering that gallium and aluminum are considered intermediate glass formers, their separation from the gallophosphate network would be expected to decrease the ability of the network to form a glass, progressively weakening the network until it can no longer be formed using standard preparation methods. However, aluminophosphate glasses with Al contents as high as P/Al = 0.5 have been prepared by sol-gel techniques.[52]

4.2- Structure-property relations

The structural development of gallophosphate glasses proposed on the basis of these spectroscopic results illuminates some of the properties measured as a function of gallium content. The T_g and T_x data shown in Figure 1b can be viewed as having three distinct regions which correlate with the structural regimes identified above. Up to 12 mol% Ga_2O_3, the addition of high-coordinate Ga effectively cross-links the nominally one-dimensional phosphate chains, progressively replacing P-O$^-$Na$^+$ by the stronger P-O-$^{[5/6]}$Ga bonds, thereby increasing the network connectivity and consequently T_g and T_x, similar to that reported for sodium aluminophosphate glasses.[55] Between 12 to 25 mol% Ga_2O_3, the increases in T_g and T_x are smaller, reflecting the fact that the added gallium is predominantly being incorporated into the phosphate chains which has little impact on the dimensionality. Within this composition range, the principal modification to the glass structure is the shortening of the phosphate chains and the introduction of gallium in tetrahedral sites. The small increase in T_g observed over this compositional region is likely due to the increased network connectivity conferred upon the glass by the coordination of these gallium cations to four network formers via bridging oxygens and also the decrease of the sodium content. Above 25 mol% Ga_2O_3, the sharp increase in T_g and T_x

Journal of Materials Chemistry C Accepted Manuscript

may be partly related to the decrease in the number of Na-O ionic bonds due to the continuous decrease of the sodium concentration in the glass skeleton formed by alternating GaO_4 and PO_4 tetrahedra as well as to the continual formation of P-O-$^{[6]}$Ga. This evolution can be compared to the first region in Figure 1b up to 12 mol% Ga_2O_3. Brow at al. have reported similar T_g behaviour in Al_2O_3-$NaPO_3$ glasses[6] however the density and refractive index profiles they report first increase and then decrease with increasing Al_2O_3 content. This different behaviour can be explained by the smaller size of Al^{3+} vis-à-vis Ga^{3+} with respect to the other constituents in the glass and illustrates the influence of density on the glass linear refractive index, since it is related to the volume fraction of the polarisable cations.

The increases in density and refractive indices with Ga_2O_3 concentration are a result of the higher molar mass, larger atomic radius and higher average coordination number of Ga^{3+} relative to the other ions in the system. Subtle features in these curves may possibly be related to the different structural roles played by gallium with increased loading. After the addition of 15 to 20 mol% Ga_2O_3, a change of slope can be observed with a much smaller increase of the density and the refractive indices as a function of Ga_2O_3 loading. This effect is likely related to the formation of a less dense gallophosphate network comprising alternating PO_4 and GaO_4 units with the presence of the excess of gallium cations in octahedral sites.

The spectral invariance of the uv-visible absorption coefficients (Figure 2a) with Ga_2O_3 concentration - except for the absorption band at 250 nm attributed to the presence of transition-metal impurities - suggests that the optical band gap is not governed by the Ga_2O_3 content, the band gap of which is close to that of $NaPO_3$ ($Eg \approx 5$ eV [56,57]), but by the relative content of bridging and non-bridging oxygens,[58] precluding an unambiguous interpretation. Similar complex behaviour of the optical band gap has been reported in sodium aluminophosphate glasses.[59]

5- Conclusions

In this work, the structure and properties of glasses belonging to the pseudo-binary $(Ga_2O_3)_x$ - $(NaPO_3)_{100-x}$ system with x varying from 0 to 32 mol% were investigated. As expected, an increase in Ga_2O_3 concentration results in an increase in glass density, linear refractive index and glass transition temperature. In contrast, no significant change in the glass short wavelength cut-off, i.e. the glass optical band gap, is observed. The complementarity of vibrational and multinuclear MAS NMR spectroscopies supports a structural model for glass formation which

Journal of Materials Chemistry C Accepted Manuscript

features three distinct roles for the gallium cations. At low loadings the gallium enters the network almost entirely as $^{[5/6]}$Ga coordinated to oxygens located on different phosphate chains, serving to increase the dimensionality and strengthen the network. Once the available coordination sites are saturated, excess gallium replaces phosphorus within the chains in a charge-ordered fashion, adopting four-coordinate geometry and introducing additional branching to the chains. Only when Ga-O-Ga bonds cannot be avoided do they begin to form, signaling the end of the glass-forming region. These distinct structural regimes correlate with specific features in the glass-transition temperatures, revealing diverse roles for gallium in influencing the glass properties. Correlations with other properties are less well defined, but exhibit patterns which suggest that the coordination environment of gallium is a key factor in determining the physical properties. While there is a substantial degree of congruence between the structural and property characteristics of gallo- and aluminophosphate glasses, key differences hint at specific advantages of gallium that may be profitably harnessed in optical applications. Hence, this study shows that while the integration of a heavy ion like gallium results in predictable increases in key properties, a closer examination of its specific structural role in the network is required to fully understand the details of its impact on the properties. This work opens the door to further studies on rare-earth doped gallophosphate glasses and their potential use in high-performance miniaturized optical devices.

Acknowledgements

The authors are grateful to the Région Aquitaine (France) and the Canadian Excellence Research Chair program (CERC - Canada) on Enabling Photonic Innovations for Information and Communication for the financial support. The Natural Sciences and Engineering Research Council of Canada (NSERC), the Fonds Québecois de la Recherche sur la Nature et les Technologies (FQRNT) and the Canada Foundation for Innovation (CFI) agencies are also acknowledged. Access to the 900 MHz NMR spectrometer was provided by the National Ultrahigh-Field NMR Facility for Solids (Ottawa, Canada), a national research facility funded by the Canada Foundation for Innovation, the Ontario Innovation Trust, Recherche Quebec, the National Research Council Canada, and Bruker BioSpin and managed by the University of Ottawa (www.nmr900.ca). The Natural Sciences and Engineering Research Council of Canada

Journal of Materials Chemistry C Accepted Manuscript

(NSERC) is acknowledged for a Major Resources Support grant. We are grateful to Dr. V.V. Terskikh for valuable assistance with the ultrahigh-field NMR experiments.

References

(1) Campbell, J. H.; Suratwala, T. I.: Nd-doped phosphate glasses for high-energy/high-peak-power lasers. *Journal of Non-Crystalline Solids* **2000**, *263&264*, 318-341.

(2) Vallet-Regi, M.; Ragel, C. V.; Salinas, A. J.: Glasses with medical applications. *European Journal of Inorganic Chemistry* **2003**, 1029-1042.

(3) Garcia, A.; Cicuendez, M.; Izquierdo-Barba, I.; Arcos, D.; Vallet-Regi, M.: Essential role of calcium phosphate heterogeneities in 2D-hexagonal and 3D-cubic SiO_2-CaO-P_2O_5 mesoporous bioactive glasses. *Chemistry of Materials* **2009**, *21*, 5474-5484.

(4) Jiang, S. B.; Myers, M.; Peyghambarian, N.: Er^{3+} doped phosphate glasses and lasers. *Journal of Non-Crystalline Solids* **1998**, *239*, 143-148.

(5) Campbell, J. H.; Hayden, J. S.; Marker, A.: High-power solid-state lasers: a laser glass perspective. *International Journal of Applied Glass Science* **2011**, *2*, 3-29.

(6) Brow, R. K.: Nature of Alumina in Phosphate-Glass: I. Properties of Sodium Aluminophosphate glass. *Journal of the American Ceramic Society* **1993**, *76*, 913-918.

(7) Subramanian, A. Z.; Murugan, G. S.; Zervas, M. N.; Wilkinson, J. S.: Spectroscopy, Modeling, and Performance of Erbium-Doped Ta_2O_5 Waveguide Amplifiers. *J. Lightwave Technol.* **2012**, *30*, 1455-1462.

(8) Kik, P. G.; Polman, A.: Erbium-Doped Optical-Waveguide Amplifiers on Silicon. *MRS Bulletin* **1998**, *23*, 48-54.

(9) Hwang, B.-C.; Jiang, S.; Luo, T.; Watson, J.; Sorbello, G.; Peyghambarian, N.: Cooperative upconversion and energy transfer of new high Er^{3+} and Yb^{3+} Er^{3+} doped phosphate glasses. *J. Opt. Soc. Am. B* **2000**, *17*, 833-839.

(10) Arai, K.; Namikawa, H.; Kumata, K.; Honda, T.; Ishii, Y.; Handa, T.: Aluminum or phosphorus co-doping effects on the fluorescence and structural properties of neodymium-doped silica glass. *Journal of Applied physics* **1986**, *59*, 3430-3436.

(11) Scheffler, M.; Kirchhof, J.; Kobelke, J.; Schuster, K.; Schwuchow, A.: Increased rare earth solubility in As–S glasses. *Journal of Non-Crystalline Solids* **1999**, *256–257*, 59-62.

Journal of Materials Chemistry C Accepted Manuscript

(12) Massera, J.; Bourhis, K.; Petit, L.; Couzi, M.; Hupa, L.; Hupa, M.; Videau, J. J.; Cardinal, T.: Effect of the glass composition on the chemical durability of zinc-phosphate-based glasses in aqueous solutions. *Journal of Physics and Chemistry of Solids* **2013**, *74*, 121-127.

(13) Choi, J.; Bellec, M.; Royon, A.; Bourhis, K.; Papon, G.; Cardinal, T.; Canioni, L.; Richardson, M.: Three-dimensional direct femtosecond laser writing of second-order nonlinearities in glass. *Optics Letters* **2012**, *37*, 1029-1031.

(14) Dussauze, M.; Fargin, E.; Lahaye, M.; Rodriguez, V.; Adamietz, F.: Large second-harmonic generation of thermally poled sodium borophosphate glasses. *Opt. Express* **2005**, *13*, 4064-4069.

(15) Brow, R. K.: Review: the structure of simple phosphate glasses. *Journal of Non-Crystalline Solids* **2000**, *263*, 1-28.

(16) Ilieva, D.; Jivov, B.; Bogachev, G.; Petkov, C.; Penkov, I.; Dimitriev, Y.: Infrared and raman spectra of Ga_2O_3-P_2O_5 glasses. *Journal of Non-Crystalline Solids* **2001**, *283*.

(17) Belkebir, A.; Rocha, J.; Esculcas, A. P.; Berthet, P.; Poisson, S.; Gilbert, B.; Gabelica, Z.; Llabres, G.; Wijzen, F.; Rulmont, A.: Structural characterization of glassy phases in the system Na_2O-Ga_2O_3-P_2O_5 by MAS-NMR, EXAFS and vibrational spectroscopy. I. Cation coordination. *Spectrochimica Acta. Part A, Molecular and biomolecular spectroscopy* **2000**, *56*, 423-34.

(18) Belkebir, A.; Rocha, J.; Esculcas, A. P.; Berthet, P.; Gilbert, B.; Gabelica, Z.; Llabres, G.; Wijzen, F.; Rulmont, A.: Structural characterization of glassy phases in the system Na_2O-Ga_2O_3-P_2O_5 by MAS and solution NMR and vibrational spectroscopy. II. Structure of the phosphate network. *Spectrochimica Acta Part A - Molecular and Biomolecular Spectroscopy* **2000**, *56*, 435-46.

(19) Brow, R. K.; Kirkpatrick, R. J.; Turner, G. L.: Nature of alumina in phosphate glass: II, structure of sodium aluminophosphate glass. *Journal of the American Ceramic Society* **1993**, *76*, 919-928.

(20) Eckert, H.: Structural characterization of noncrystalline solids and glasses using solid-state NMR. *Progress in Nuclear Magnetic Resonance Spectroscopy* **1992**, *24*, 159-293.

(21) MacKenzie, K. J. D.; Smith, M. E.: *Multinuclear Solid-State Nuclear Magnetic Resonance of Inorganic Materials*; Pergamon, 2002; Vol. 6.

Journal of Materials Chemistry C Accepted Manuscript

(22) Kroeker, S. in *Modern Glass Characterization*; ed. M. Affatigato, Wiley-American Ceramic Society, in press.

(23) Miyaji, F.; Tadanaga, K.; Yoko, T.; Sakka, S.: Coordination of Ga^{3+} ions in PbO-Ga_2O_3 glasses as determined by ^{71}Ga NMR. *Journal of Non-Crystalline Solids* **1992**, *139*, 268-270.

(24) Randall, E.; Youngman; Aitken, B. G.: Structure and properties of GeGaP sulfide glasses. *Journal of Non-Crystalline Solids* **2004**, *345&346*, 50-55.

(25) Stebbins, J. F.; Du, L. S.; Kroeker, S.; Neuhoff, P.; Rice, D.; Frye, J.; Jakobsen, H. J.: New opportunities for high-resolution solid-state NMR spectroscopy of oxide materials at 21.1 and 18.8T fields. *Solid State Nucl Mag* **2002**, *21*, 105-115.

(26) Kamitsos, E. I.; Yiannopoulos, Y. D.; Varsamis, C. P. E.; Jain, H.: Structure-property correlation in glasses by infrared reflectance spectroscopy. *J. Non-Cryst. Solids* **1997**, *222*, 59.

(27) Kamitsos, E. I.: Comment on Infrared-reflectance spectra of heat-treated, sol-gel-derived silica. *Phys. Rev. B* **1996**, *53*, 14659.

(28) Massiot, D.; Fayon, F.; Capron, M.; King, I.; Le Calve, S.; Alonso, B.; Durand, J. O.; Bujoli, B.; Gan, Z. H.; Hoatson, G.: Modelling one- and two-dimensional solid-state NMR spectra. *Magn Reson Chem* **2002**, *40*, 70-76.

(29) Neuville, D. R.; Cormier, L.; Massiot, D.: Al environment in tectosilicate and peraluminous glasses: a Al-27 MQ-MAS NMR, Raman, and XANES investigation. *Geochimica et Cosmochimica Acta* **2004**, *68*, 5071-5079.

(30) Ehrt, D.; Ebeling, P.; Natura, U.: UV Transmission and radiation-induced defects in phosphate and fluoride-phosphate glasses. *Journal of Non-Crystalline Solids* **2000**, *263*, 240-250.

(31) Shelby, J. E.; Slilaty, R. M.: Calcium gallioaluminate glasses. *Journal of Applied Physics* **1990**, *68*, 3207-3211.

(32) Peng, L.; Stebbins, J. F.: High resolution ^{17}O MAS and triple-quantum MAS NMR studies of gallosilicate glasses. *Journal of Non-Crystalline Solids* **2008**, *354*, 3120-3128.

(33) Varshneya, A. K.: *Fundamentals of Inorganic Glasses*; Academic Press Inc: Boston, 1994.

Journal of Materials Chemistry C Accepted Manuscript

(34) Angot, E.; Le Parc, R.; Levelut, C.; Beaurain, M.; Armand, P.; Cambon, O.; Haines, J.: A high-temperature Raman scattering study of the phase transitions in $GaPO_{(4)}$ and in the $AlPO_{(4)}$-$GaPO_{(4)}$ system. *Journal of Physics-Condensed Matter* **2006**, *18*, 4315-4327.

(35) Velli, L. L.; Varsamis, C. P. E.; Kamitsos, E. I.; Moncke, D.; Ehrt, D.: Structural investigation of metaphosphate glasses. *Physics and Chemistry of Glasses* **2005**, *46*, 178-181.

(36) Dussauze, M.; Rodriguez, V.; Velli, L.; Varsamis, C. P. E.; Kamitsos, E. I.: Polarization mechanisms and structural rearrangements in thermally poled sodium-alumino phosphate glasses. *Journal of Applied Physics* **2010**, *107*.

(37) Hudgens, J. J.; Brow, R. K.; Tallant, D. R.; Martin, S. W.: Raman spectroscopy study of the structure of lithium and sodium ultraphosphate glasses. *Journal of Non-Crystalline Solids* **1998**, *223*, 21-31.

(38) Zhao, Y.; Frost, R. L.: Raman spectroscopy and characterisation of α-gallium oxyhydroxide and β-gallium oxide nanorods. *Journal of Raman Spectroscopy* **2008**, *39*, 1494-1501.

(39) Dohy, D.; Lucazeau, G.; Revcolevschi, A.: Raman-spectra and valence force-field of single-crystalline β-Ga_2O_3. *Journal of Solid State Chemistry* **1982**, *45*, 180-192.

(40) Fukunaga, J.; Bando, R.; Ota, R.; Yoshida, N.: Raman Spectra and Structure of Glasses in the System Na_2O-Ga_2O_3-B_2O_3. *Journal of the Ceramic Society of Japan* **1988**, *96*, 634-638.

(41) Miyaji, F.; Sakka, S.: Structure of PbO-Bi_2O_3-Ga_2O_3 glasses. *Journal of Non-Crystalline Solids* **1991**, *134*, 77-85.

(42) Pickup, D. M.; Valappil, S. P.; Mos, R. M.; Twyman, H. L.; Guerry, P.; Smith, M. E.; Wilson, M.; Knowles, J. C.; Newport, R. J.: Preparation, structural characterisation and antibaterial properties of Ga-doped sol-gel phosphate-based glass. *J. Mater. Sci.* **2009**, *44*, 1858-1867.

(43) Massiot, D.; Farnan, I.; Gautier, N.; Trumeau, D.; Trokiner, A.; Coutures, J. P.: ^{71}Ga and ^{69}Ga nuclear magnetic resonance study of β-Ga_2O_3: resolution of four- and six-fold coordinated Ga sites in static conditions. *Solid State Nucl Mag* **1995**, *4*, 241-248.

(44) Ash, J. T.; Grandinetti, P. J.: Solid-state NMR characterization of ^{69}Ga and ^{71}Ga in crystalline solids. *Magn Reson Chem* **2006**, *44*, 823-831.

Journal of Materials Chemistry C Accepted Manuscript

(45) Bradley, S. M.; Howe, R. F.; Kydd, R. A.: Correlation between ^{27}Al NMR and ^{71}Ga NMR Chemical-Shifts. *Magn Reson Chem* **1993**, *31*, 883-886.

(46) Massiot, D.; Vosegaard, T.; Magneron, N.; Trumeau, D.; Montouillout, V.; Berthet, P.; Loiseau, T.; Bujoli, B.: ^{71}Ga NMR of reference Ga-IV, Ga-V, and Ga-VI compounds by MAS and QPASS, extension of gallium/aluminum NMR parameter correlation. *Solid State Nucl Mag* **1999**, *15*.

(47) Neuville, D. R.; Cormier, L.; Massiot, D.: Al coordination and speciation in calcium aluminosilicate glasses: Effects of composition determined by Al-27 MQ-MAS NMR and Raman spectroscopy. *Chemical Geology* **2006**, *229*, 173-185.

(48) Stebbins, J. F.; Dubinsky, E. V.; Kanehashi, K.; Kelsey, K. E.: Temperature effects on non-bridging oxygen and aluminum coordination number in calcium aluminosilicate glasses and melts. *Geochimica Et Cosmochimica Acta* **2008**, *72*, 910-925.

(49) Farnan, I.; Stebbins, J. F.: The nature of the glass transition in a silica-rich oxide melt. *Science* **1994**, *265*, 1206-1209.

(50) Egan, J. M.; Wenslow, R. M.; Mueller, K. T.: Mapping aluminum/phosphorus connectivities in aluminophosphate glasses. *Journal of Non-Crystalline Solids* **2000**, *261*, 115-126.

(51) Lang, D. P.; Alam, T. M.; Bencoe, D. N.: Solid-state ^{31}P/^{27}AI and ^{31}P/^{23}Na TRAPDOR NMR investigations of the phosphorus environments in sodium aluminophosphate glasses. *Chemistry of Materials* **2001**, *13*, 420-428.

(52) Zhang, L.; Eckert, H.: Sol-gel synthesis of Al_2O_3-P_2O_5 glasses: Mechanistic studies by solution and solid state NMR. *Journal of Materials Chemistry* **2004**, *14*, 1605-1615.

(53) Brow, R. K.; Kirkpatrick, R. J.; Turner, G. L.: The short range structure of sodium phosphate glasses I. MAS NMR studies. *Journal of Non-Crystalline Solids* **1990**, *116*, 39-45.

(54) Vandermeer, H.: The crystal structure of a monoclinic form of aluminium metaphosphate, $Al(PO_3)_3$. *Acta Crystallographica Section B* **1976**, *32*, 2423-2426.

(55) Schneider, J.; Oliveira, S. L.; Nunes, L. A. O.; Panepucci, H.: Local structure of sodium aluminum metaphosphate glasses. *Journal of the American Ceramic Society* **2003**, *86*, 317-324.

Journal of Materials Chemistry C Accepted Manuscript

(56) Lu, J. G.; Chang, P. C.; Fan, Z. Y.: Quasi-one-dimensional metal oxide materials - Synthesis, properties and applications. *Materials Science & Engineering R-Reports* **2006**, *52*, 49-91.

(57) Subrahmanyam, K.; Salagram, M.: Optical band gap studies on (55-x)Na_2O-xPbO-45P_2O_5 (SLP) glass system. *Optical Materials* **2000**, *15*, 181-186.

(58) Bach, H.; N., N.: *The properties of optical glass*; Springer: New York, 1995.

(59) Shah, K. V.; Sudarsan, V.; Goswami, M.; Sarkar, A.; Manikandan, S.; Kumar, R.; Sharma, B. I.; Shrikhande, V. K.; Kothiyal, G. P.: Preparation and studies of some thermal, mechanical and optical properties of xAl_2O_3 (1-x)$NaPO_3$ glass system. *Bulletin of Materials Science* **2003**, *26*, 715-720.

Journal of Materials Chemistry C Accepted Manuscript

Table captions

Table 1. Comparison between experimental and theoretical elemental compositions of the Ga_2O_3-$NaPO_3$ glasses

Table 2. Proposed Raman and infrared band assignments for the gallophosphate glasses

Journal of Materials Chemistry C Accepted Manuscript

Table 1. Comparison between experimental and theoretical elemental compositions of the Ga_2O_3-$NaPO_3$ glasses

Sample label	Ga_2O_3 (mol%)		Na_2O (mol%)		P_2O_5 (mol%)		Ga_2O_3/P_2O_5		Na_2O/P_2O_5	
	Theo.	Expt. (±0.2)	Theo.	Expt. (±0.2)	Theo.	Expt. (±0.2)	Theo.	Expt. (±0.02)	Theo.	Expt. (±0.02)
Ga0	0.0	**0.0**	50.0	**51.6**	50.0	**48.4**	0.00	**0.00**	1.00	**1.07**
Ga5	5.0	**5.3**	47.5	**49.2**	47.5	**45.5**	0.11	**0.12**	1.00	**1.08**
Ga12	10.0	**12.1**	45.0	**45.0**	45.0	**42.9**	0.22	**0.28**	1.00	**1.05**
Ga15	15.0	**15.5**	42.5	**42.4**	42.5	**42.1**	0.35	**0.37**	1.00	**1.01**
Ga22	20.0	**21.6**	40.0	**39.5**	40.0	**38.9**	0.50	**0.56**	1.00	**1.02**
Ga25	25.0	**25.4**	37.5	**38.9**	37.5	**35.7**	0.67	**0.71**	1.00	**1.09**
Ga29	27.5	**29.3**	36.3	**36.8**	36.3	**33.9**	0.76	**0.86**	1.00	**1.09**
Ga32	30.0	**31.8**	35.0	**35.6**	35.0	**32.6**	0.86	**0.98**	1.00	**1.09**

Journal of Materials Chemistry C Accepted Manuscript

Table 2. Proposed Raman and infrared bands assignment for the gallophosphate glasses

Peak position	Raman bands assignment	Infrared bands assignment	Ref.
500 cm^{-1}	GaO_4 bending		40
~ 590 cm^{-1}		GaO_6 vibration mode and O-P-O deformation mode	41,42
~ 640 cm^{-1}	GaO_4 stretching vibrations	vibrational mode of GaO_4 tetrahedra	17,18,38-40
~ 690 cm^{-1}	P-O-P bonds sym. stretching vibrations with Q^2		15,18
~ 750 cm^{-1}	P-O-P bonds stretching vibrations with Q^1		15-18
~ 880 cm-1		asym. vibrations of P-O-P chains with Q^2 units	35
~920 cm^{-1}	sym. PO_4 stretching in Q^0 vibrations + asym. P-O-P vibrations	vibrations related to P-O-P bonds	15,17,18,35
~1000-1050 cm^{-1}	sym. vibrations of ($ØPO_3^{2-}$) Q^1 species	P-O-P asym. vibrations and sym. stretching mode of end groups ($ØPO_3^{2-}$) Q^1 units	15,18,35
~1100 cm^{-1}	(sym. PO_2 stretch in Q^2) + asym. of ($ØPO_3^{2-}$) Q^1vibrations	asym. stretching mode of end groups ($ØPO_3^{-}$) Q^1 units	12,35
~1150 cm^{-1}	($PØ_2O_2^{-}$) Q^2 symmetric stretch vibrations	Q^2	15,18,35
1200-1230 cm^{-1}	asym. PO_2 stretch in Q^2 vibrations		15
~1270 cm-1	(P=O) sym. Q^3 stretching	Q^2 and Q^3 units	35,37

Journal of Materials Chemistry C Accepted Manuscript

Figure captions

Figure 1. (a) Density and (b) glass transition and crystallization onset temperatures of the Ga_2O_3-$NaPO_3$ glasses as a function of Ga_2O_3 content. Lines are guides for the eye.

Figure 2. (a) Absorption coefficient spectra in the short-wavelength region and (b) linear refractive indices measured at 532, 633, 972, 1308 and 1538 nm of the Ga_2O_3-$NaPO_3$ glasses as a function of the Ga_2O_3 content. Lines are guides for the eye.

Figure 3. Schematic representations of the P and Ga short-range order structural units in sodium gallophosphate glasses

Figure 4. Normalized Raman spectra (a) and normalized infrared spectra (b) of the Ga_2O_3-$NaPO_3$ glass samples as a function of the Ga_2O_3 content.

Figure 5. ^{71}Ga MAS NMR spectra obtained at 21.1 T and 60 kHz spinning speed of Ga_2O_3-$NaPO_3$ glasses as a function of the Ga_2O_3 concentration

Figure 6. (a) Experimental and calculated ^{71}Ga MAS NMR spectra of Ga22, with subspectral fits for $^{[4]}$Ga, $^{[5]}$Ga, $^{[6]}$Ga; (b) integrated NMR intensities of $^{[4]}$Ga, $^{[5]}$Ga and $^{[6]}$Ga; (c) $^{[4]}$Ga, $^{[5]}$Ga and $^{[6]}$Ga concentration with respect to total SRO units in the glass; (d) ^{71}Ga isotropic chemical shift of $^{[4]}$Ga, $^{[5]}$Ga and $^{[6]}$Ga. All lines are spline fits intended as guides for the eye.

Figure 7. ^{31}P MAS NMR spectra of the Ga_2O_3-$NaPO_3$ glasses as a function of Ga_2O_3 concentration.

Figure 8. Schematic representations of the structural roles of $^{[6]}$Ga and $^{[4]}$Ga in Ga_2O_3-$NaPO_3$ glasses

Journal of Materials Chemistry C Accepted Manuscript

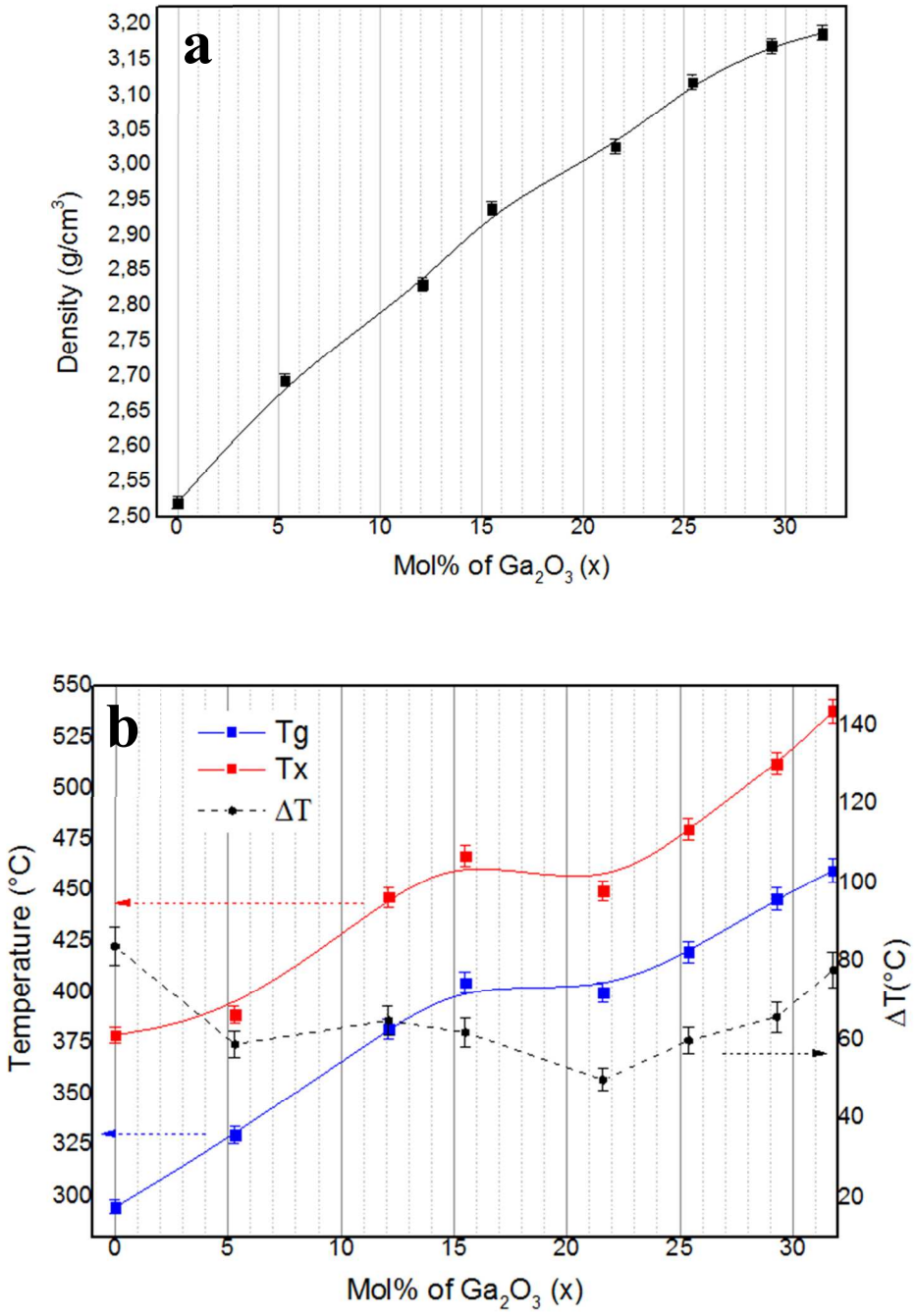

Figure 1. (a) Density and (b) glass transition and crystallization onset temperatures of the Ga_2O_3-$NaPO_3$ glasses as a function of Ga_2O_3 content. Lines are guides for the eye.

Journal of Materials Chemistry C Accepted Manuscript

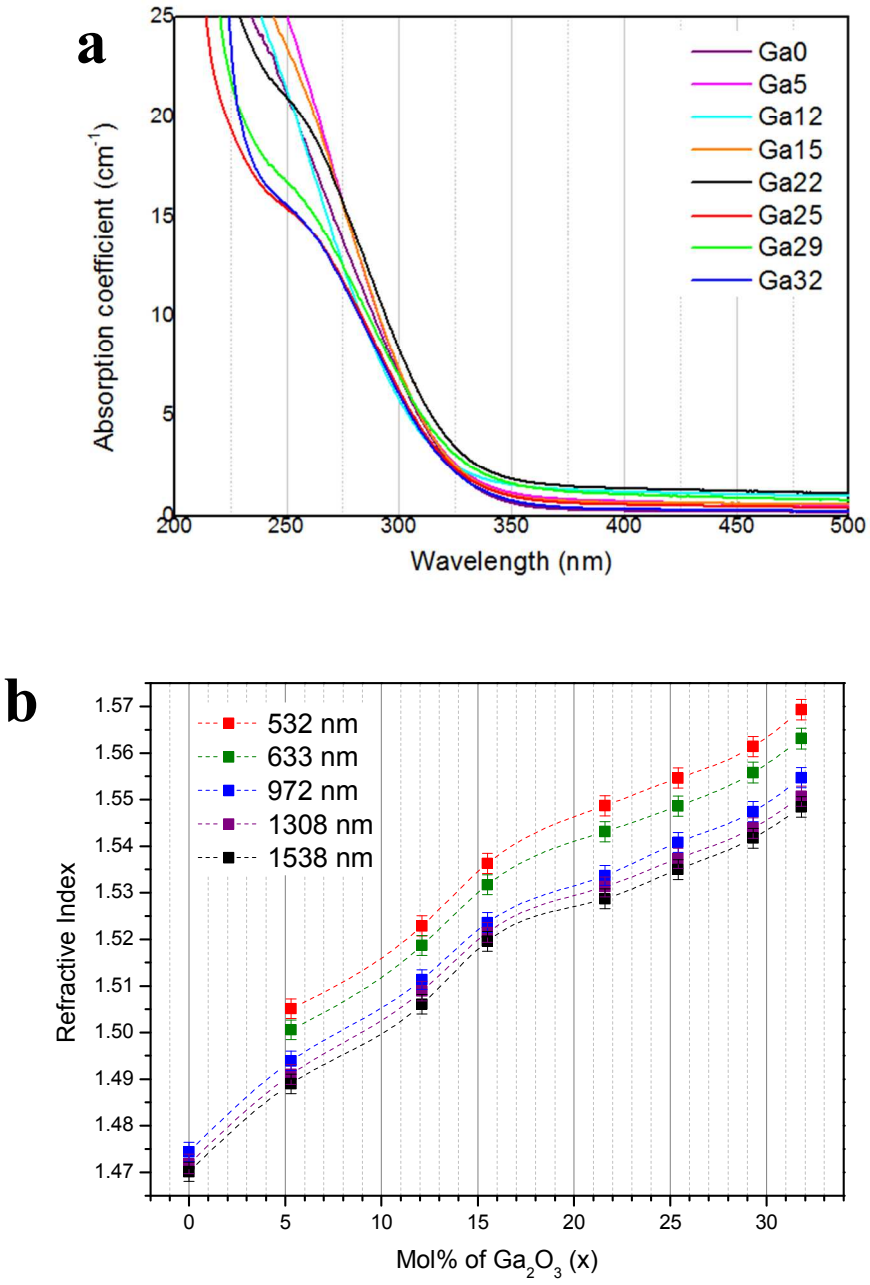

Figure 2. (a) Absorption coefficient spectra in the short-wavelength region and (b) linear refractive indices measured at 532, 633, 972, 1308 and 1538 nm of the Ga_2O_3-$NaPO_3$ glasses as a function of the Ga_2O_3 content. Lines are guides for the eye.

Journal of Materials Chemistry C Accepted Manuscript

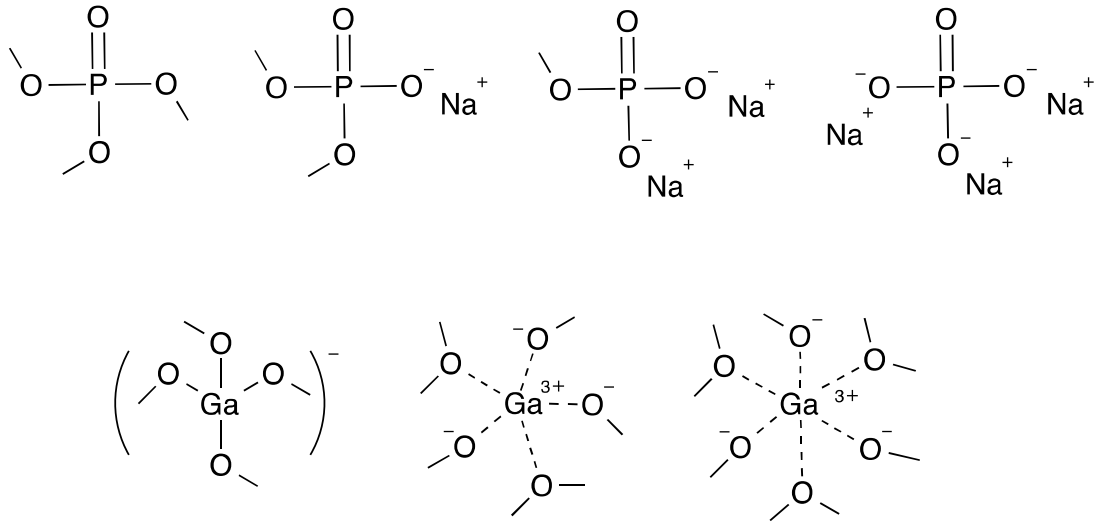

Figure 3. Schematic representations of the P and Ga short-range order structural units in sodium gallophosphate glasses

Journal of Materials Chemistry C Accepted Manuscript

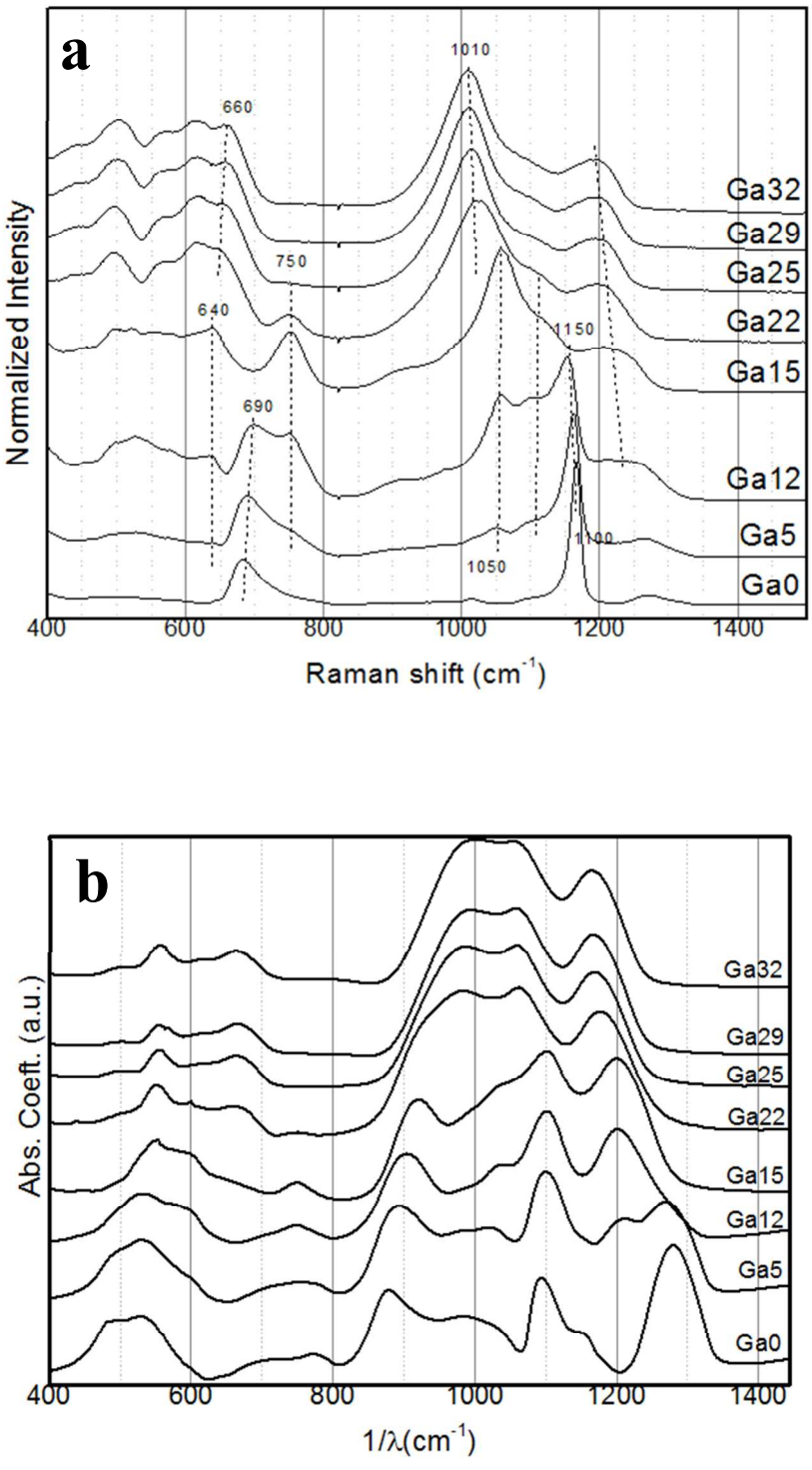

Figure 4. Normalized Raman spectra (a) and normalized infrared spectra (b) of the Ga_2O_3-$NaPO_3$ glass samples as a function of the Ga_2O_3 content.

Journal of Materials Chemistry C Accepted Manuscript

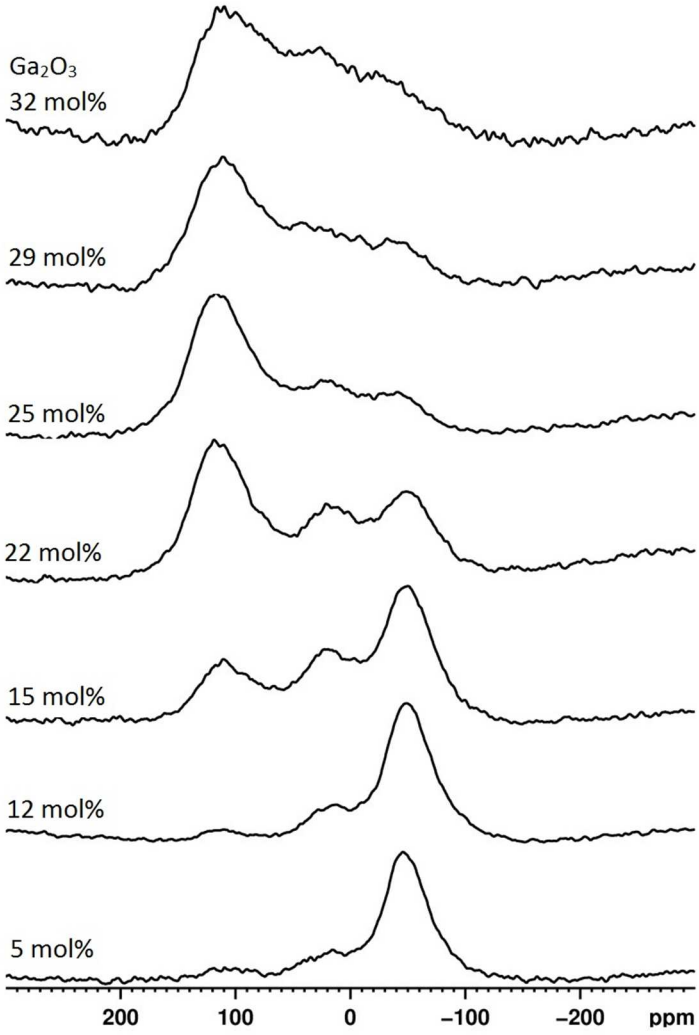

Figure 5. ^{71}Ga MAS NMR spectra obtained at 21.1 T and 60 kHz spinning speed of Ga_2O_3-$NaPO_3$ glasses as a function of the Ga_2O_3 concentration

Journal of Materials Chemistry C Accepted Manuscript

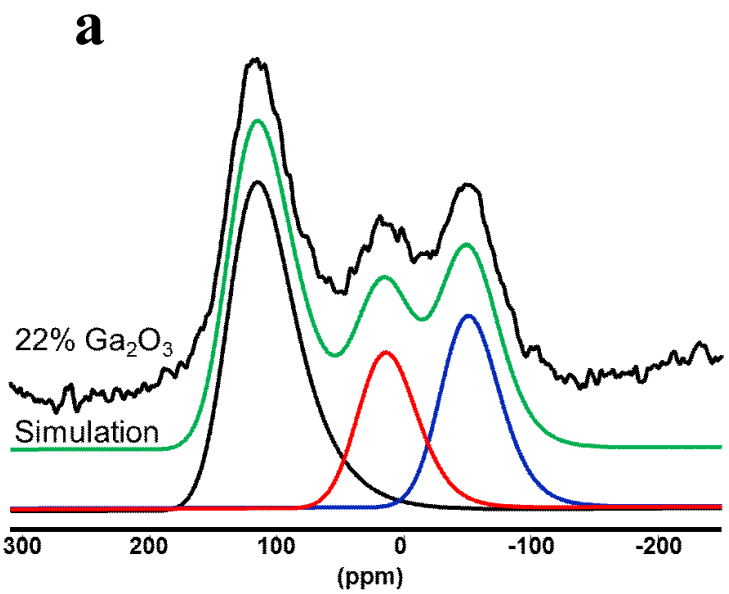

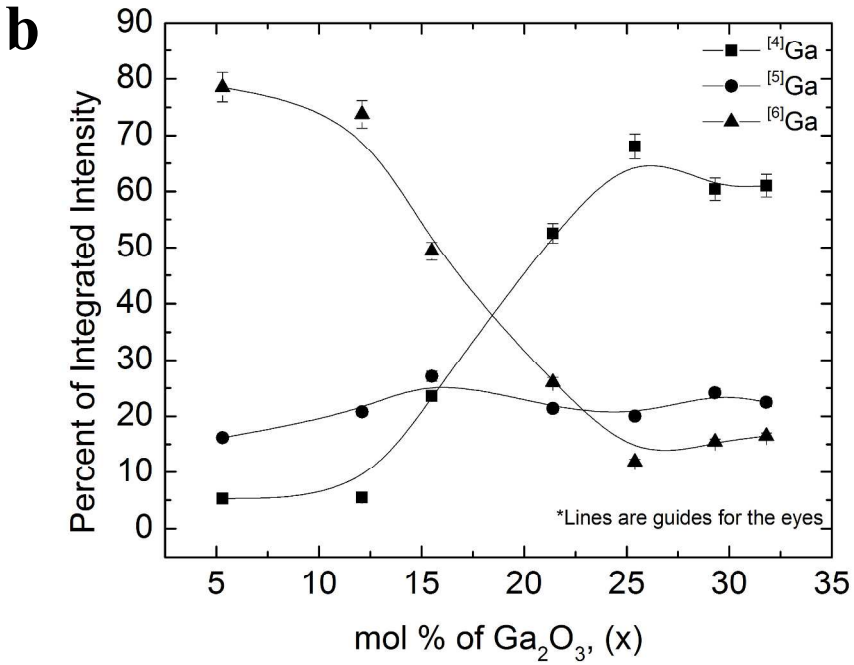

Journal of Materials Chemistry C Accepted Manuscript

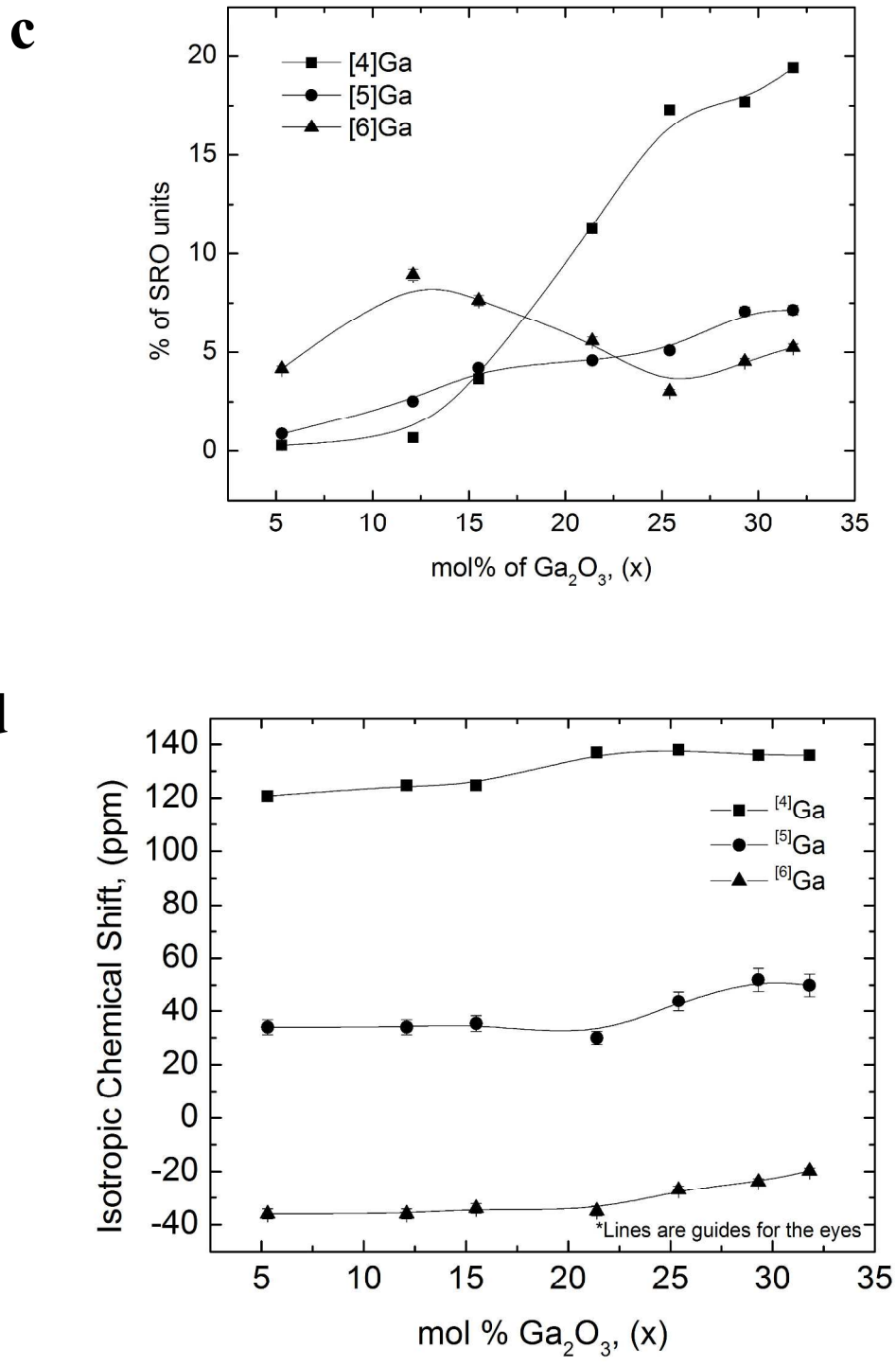

Figure 6. (a) Experimental and calculated ^{71}Ga MAS NMR spectra of Ga22, with subspectral fits for $^{[4]}$Ga, $^{[5]}$Ga, $^{[6]}$Ga; (b) integrated NMR intensities of $^{[4]}$Ga, $^{[5]}$Ga and $^{[6]}$Ga; (c) $^{[4]}$Ga, $^{[5]}$Ga and $^{[6]}$Ga concentration with respect to total SRO units in the glass; (d) ^{71}Ga isotropic chemical shift of $^{[4]}$Ga, $^{[5]}$Ga and $^{[6]}$Ga. All lines are spline fits intended as guides for the eye.

Journal of Materials Chemistry C Accepted Manuscript

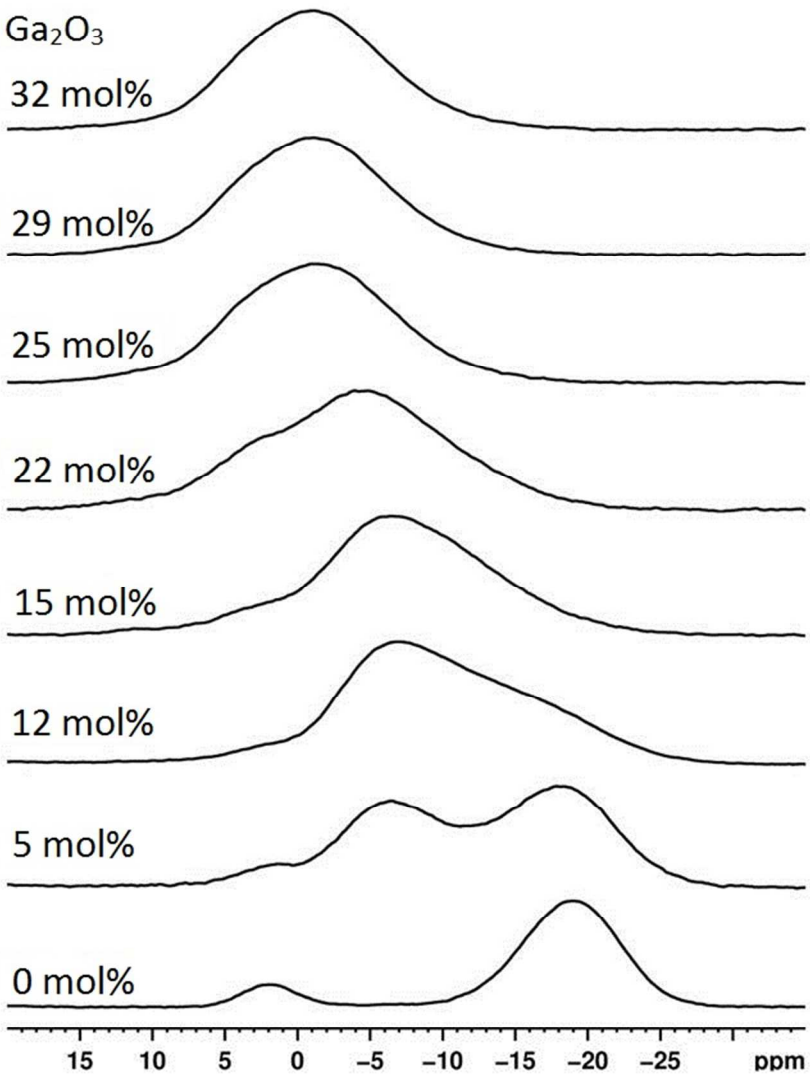

Figure 7. ^{31}P MAS NMR spectra of the Ga_2O_3-$NaPO_3$ glasses as a function of Ga_2O_3 concentration.

Journal of Materials Chemistry C Accepted Manuscript

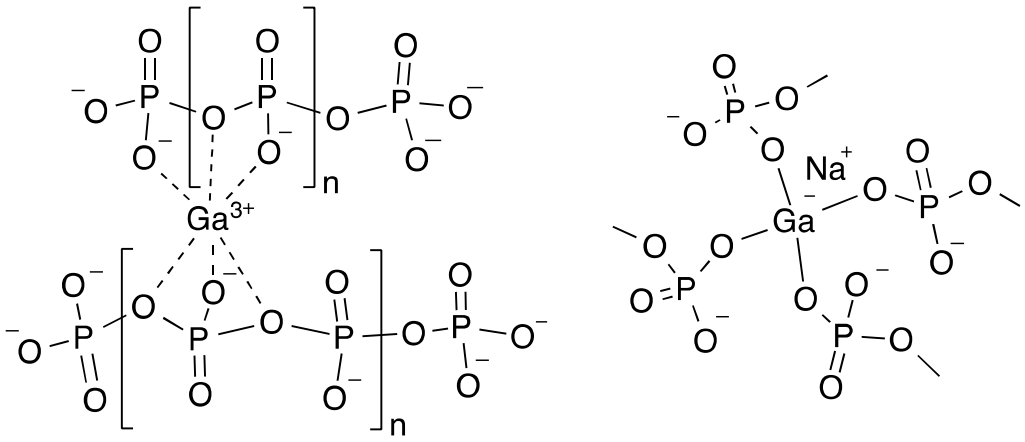

Figure 8. Schematic representations of the structural roles of $^{[6]}$Ga and $^{[4]}$Ga in Ga_2O_3-$NaPO_3$ glasses

Journal of Materials Chemistry C Accepted Manuscript